ISSN 1063-7834, Physics of the Solid State, 2018, Vol. 60, No. 7, pp. 1458–1461. © Pleiades Publishing, Ltd., 2018.
Original Russian Text © V.M. Egorov, V.A. Marikhin, 2018, published in Fizika Tverdogo Tela, 2018, Vol. 60, No. 7, pp. 1441–1444.

Revealing Generality of the Thermodynamic Properties for Crystals of Long-Chain Aliphatics and Polymethylene

V. M. Egorov[a], * and V. A. Marikhin[a]
[a] *Ioffe Institute, St. Petersburg, Russia*
**e-mail: victor_egorov1@inbox.ru*

Received January 24, 2018

Abstract—We analyze the dependency of melting points of molecular crystals with different chain lengths on the crystal habit of elementary volume for the first-order phase transition. We demonstrate that molecular crystals with identical chemical structure of their cores—unbranched alkanes $CH_3(CH_2)_nCH_3$, diols $HOC(CH_2)_nCOH$, unbranched aliphatic alcohols $CH_3(CH_2)_nCOH$, saturated carboxylic acids $CH_3(CH_2)_nCOOH$, and dicarboxylic acids $HOOC(CH_2)_nCOOH$—lose their identity and individual properties and evolve toward polyethylene as the number of repeating $-CH_2-$ groups increases.

DOI: 10.1134/S1063783418070119

This study is the next in a series of works in which we have been investigating the effects different end-groups have on the structure and properties of long-chain molecular crystals (LCMCs). Owing to their monodespersity and a lack of chemical defects, the LCMCs are suitable model compounds for studying such arguable questions as the effects the chain length and type of end-groups have on the evolution of structure during crystallization and structural transformations at phase transitions. Studying the differences between LCMCs and ordinary polydisperse polymers with chemical defects is of particular importance in establishing generalized quantitative structure–properties relationships.

In our earlier works, we provided quantitative analyses of the phase transitions in homologous series of long-chain alkanes [1, 2], n-alcohols [3], alkane diols [4–7], mono- and dicarboxylic acids [8, 9]. The supramolecular structures of these LCMCs consist of nanocrystalline plates (lamellae) that are few nm thick, values comparable to the chain lengths, and have ordered three-dimensional cores of aligned CH_2 groups, with the plate's surface layers being constituted of different end-groups (e.g., $-CH_3$, $-OH$, and $-COOH$).

Since repeating methylene groups ($-CH_2-$) form the cores of LCMCs, these compounds can be ordered in a series in terms of the strength of interactions between the end-groups (from weaker to stronger), starting from compounds exhibiting van der Waals interactions ($-CH_3$ groups of alkanes and alcohols) and ending with members exhibiting specific interactions to form hydrogen bonds ($-COH$ groups of alcohols and diols and $-COOH$ groups of carboxylic acids). Hydroxyl end-groups cover the basal planes of lamellar crystals to form double layers and extended “polymer” chains of hydrogen bonds. This results in considerable surface energy on the end side of such crystals, and, consequently, in alteration of their thermodynamic properties including the melting point. At the same time, with the growing number of repeating $-CH_2-$ groups in the core of lamellar crystals, the crystals tend to lose their identity and their individual properties evolve toward those of polymethylene, since the energy of crystal bulk, which consists of cohesive interactions between methylene trans-chains in the crystalline cores of lamellae and is proportional to their length, increases, while the surface energy component of the indicated LCMCs remains unchanged.

The variation of melting point T_m, one of the thermodynamic characteristics of LCMCs, with n is shown in Fig 1. These are differential scanning calorimetry data for the whole set of different LCMCs with varying number of repeating $-CH_2-$ groups in their molecules. Two immediate conclusions can be drawn from these data: (1) an increase in the free energy of the end side results in elevated melting points for lamellar crystals with the same n, especially for $n \leq 20$; and (2) T_m increases with n in a nonlinear manner.

The nonlinear dependency of T_m can be explained by a size effect, which manifests for sufficiently small particles, and nanoscopic lamella of LCMCs can be attributed to this category. The differences in the phase states of small particles are dictated by various “internal” causes that are in certain relation to one another

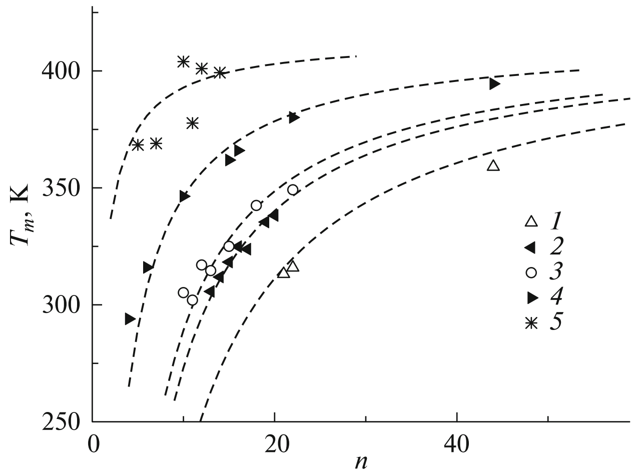

Fig. 1. Melting point T_m as a function of the number n of methlene groups –CH– for various LCMCs: (*1*) alkanes, (*2*) alcohols, (*3*) carboxylic acids, (*4*) diols, and (*5*) dicarboxylic acids.

[10–12]. The size effect in particular manifests as a shift in the phase transition temperature including the melting point. The temperature shift ΔT depends on a number of different factors and the general expression for it reads: $\Delta T/T_0 = \gamma K/\Delta H \rho R$, where γ is the surface free energy; ρ, the crystal density; ΔH, the enthalpy of phase transition; R, the characteristic size of a small particle or the thickness of a thin film; K is shape factor; and $T = T_0 - T_m$, with T_0 and T_m being the phase transition temperatures for the material in question in its bulk form and in the form of small particles.

This general expression, as applied to a LCMC, takes the form:

$$T_m = 414.5(1 - A/L), \tag{1}$$

where L is the thickness of lamella, and more specifically $L = 0.1273n$, with n being the number of carbon atoms in the chain. The factor 0.1273 (in nm) is the projection of a C–C bond on the axis of the considered molecule; and A is a parameter that accounts for the surface free energy, the density of lamella's crystalline core, and the phase transition enthalpy. Because the cores of molecular crystals are built from chains of identical methylene groups ($-CH_2-$), the two latter parameters, to the first approximation, can be taken as general ones and independent of n for the whole set of LCMCs considered in this work.

The experimental melting points for the different molecular crystals are in a satisfactory agreement with Eq. (1), as can be appreciated from Fig. 1. In so doing, the parameter A took the following values: 0.95 for dicarboxylic acids, 2.25 for diols, 4.15 for monocarboxylic acids, 4.68 for alcohols, and 7.3 for alkanes. These values for A show us that contrary to the expected increase in the surface free energy with progressively more intensive interaction between the end-groups, as Eq. (1) suggests—when the energy of interaction grows from van der Waals forces to specific interactions that give rise to different types of hydrogen bonding—we observe seemingly lower surface free energies for molecular crystals of comparable lengths. This conclusion is in line with the assumption that lamellae are the structural units of molecular crystals. If, however, the lamellae overlay preserving the long-distance crystallographic ordering in the crystal and thus giving thicker effective crystals, the effect under discussion can be rationalized by mismatch of the thickness L of a singular lamella as used in Eq. (1) for calculating the curves shown in Fig. 1 and the actual (effective) thickness L^*, which exceeds L several times.

To establish the relation between the parameters L and L^*, we must consider the energetics of phase transition and the balance between the surface energy and volume energies during nucleation of a new phase.

This has actually been accomplished earlier in a study in which the shapes of peaks on the thermal conductivity profile of the first-order solid–solid (structural) phase transition were analyzed using differential scanning calorimetry [13]. Quantitative treatment of the peak shapes was performed within the theory of smeared phase transitions enabling us to determine the volumes of heterogeneous nanonuclei of the new phase Ω that originate as a result of fluctuations at defects in the parental phase and that are responsible for advancement of the interface during the phase transition [14, 15]. It was shown that the crystal habit of LCMCs varied from nanoprisms (for n-alkanes) to nanofibrils consisting of stacks of 6–7 lamellae (for dicarboxylic acids), depending on the ratio of the surface free energy of the lateral sides to that of the end sides of crystals. This effect is caused by the characteristic symmetry of packing of molecules in lamellae and these lamellae in stacks, in addition to the formation of dimer hydrogen bonds between adjacent lamellae [13]. The actual thickness of a single lamella was found to be in line with the formula

$$L^* = \omega^{1/3}(E_{kn}/E_{k1}^{2/3}), \tag{2}$$

where E_{k1} and E_{kn} are the cohesion energies for the methylene groups and end-groups, respectively. Here we used the values for cohesive energies as quoted in work [16]: $E_{k1} = 3.6$ kJ/mol for contributions from CH_2 groups, $E_{k2} = 4.14$ kJ/mol for CH_3 groups, $E_{k3} = 13.4$ kJ/mol for hydrogen bonding involving COH groups, and $E_{k4} = 26.8$ kJ/mol for dimer hydrogen bonding in COOH groups. Taking the smallest of these values as unity for the surface energy of an alkane, we obtained the following ascending series for L^*: alkanes ($L_1^* = 1$), alcohols ($L_2^* > 1.5$), carboxylic acids ($L_3^* > 1.7$), diols ($L_4^* > 3.0$), and dicarboxylic acids ($L_5^* > 6.9$).

Shown in Fig. 2 are the variations of melting points T_m with the number n of repeating $-CH_2-$ groups in

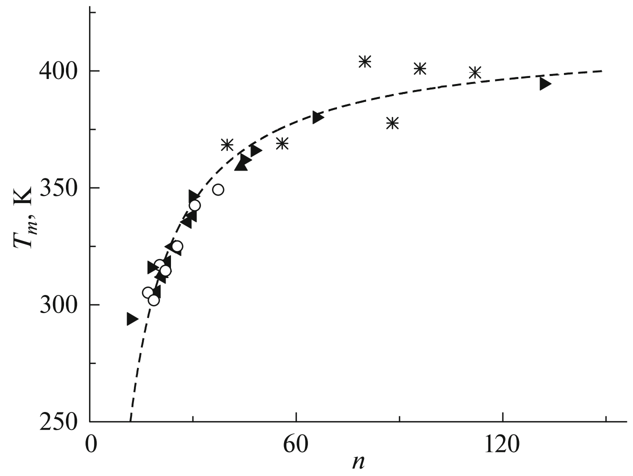

Fig. 2. Melting point T_m as a function of the number n of methylene groups –CH– in lamellae having effective thickness L^*_{1-5} for various long-chain LCMCs (designations for symbols are the same as in Fig. 1).

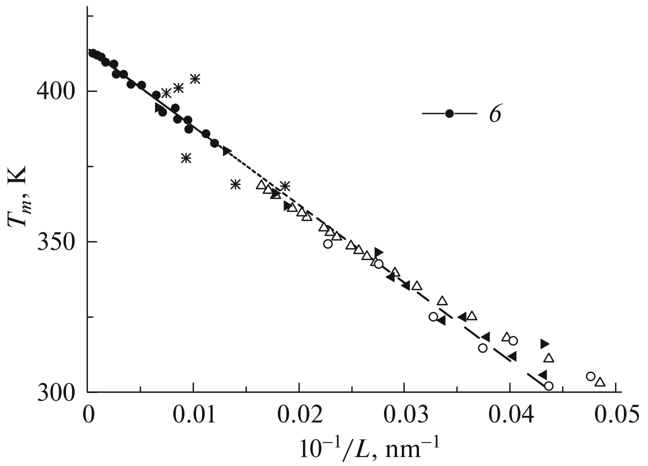

Fig. 3. Melting point T_m as a function of lamella thickness for polyethylene (*6*; data from [19]) and LCMCs (designations for other symbols are the same as in Fig. 1).

lamellae with effective thickness L^*_{1-5} for all the LCMCs considered in this study. As can be seen from the figure, the experimental data accurately fall on a single curve $T_m(n)$ that was obtained using Eq. (1) for alkanes. This means that the function $T_m = f(n)$ for which the balance between the internal and surface energies of crystalline lamellae was accounted for embraces LCMCs with different chemical structures.

As was noted above, with increasing number of repeating $-CH_2-$ groups, the LCMCs tend to lose their identity and their individual properties evolve toward those of polymethylene. The Thomson–Gibbs equation [17, 18], which is similar to Eq. (1), is commonly used in studies on melting and crystallization of polymer crystals with lamellar structure, in particular, polyethylene and polymethylene:

$$T_m = T_0[1 - 2\gamma/\Delta H_0 \rho L_0]. \tag{3}$$

The thickness of lamella L_0, free surface energy at the end side (γ), enthalpy ΔH_0, and the melting point T_0 of an infinite crystal at equilibrium are used as size-determining parameters. For polyethylene ΔH_0 = 290 J/g and T_0 = 414.5 K [19]. For lamellae having rather large cross section sizes, the surface free energy of the lateral side can be neglected because the surface of the end side is considerably larger than that of the lateral side. Because LCMCs bear the features of both small particles that are subject to the phase size effect and "polymer" lamellar supramolecular structures with nanoscopic thicknesses of the constituent lamellae, the correct application of the Thomson–Gibbs equation to molecular crystals requires, in addition to the surface free energy being accounted for, estimating the actual thicknesses L^* of effective macrocrystals, the stacks of lamellae.

The melting points of polyethylene crystals with lamellar structure were studied in work [19] for a broad range of different types of samples: some lacked orientation, while others were obtained by crystallization from a melt or a solution. These data, in the form of a T_m vs. reciprocal lamella thickness are plotted in Fig. 3. We can see that the experimental data fall on a straight line $T_m = 414.2[1 - 6.27/L_0] \pm 0.8$ K. Extrapolation of this line gives T_m = 414.2 K, which is the equilibrium melting point for crystals consisting of stretched chains of high molecular weight polyethylene.

The same figure shows the T_m data for the LCMCs plotted vs. reciprocal thickness L^*_{1-5}. These data cover considerably broader range of sizes of lamellar formations. It can be seen that the data points fall fairly well on the straight line that describes the lemallar structure of polyethylene. The greatest deviations from the straight line are observed for the LCMCs with the shortest chain lengths, including dicarboxylic acids.

These deviations seem to be related to breaking of intermolecular van der Waals forces among $-CH_2-$ groups in short chains at temperatures below T_m. This effect can be caused by end-groups (e.g., $-CH_3$, $-OH$, and $-COOH$) that create significant steric hindrances for ordered packing of methylene groups inside of lamellae thus giving rise to a peculiar, distorted layered structure. In this case, crystallization and re-establishment of van der Waals forces between the methylene groups either occurs at lower temperatures or it does takes place at all. The crystalline cores of these lamellae exist in a mesophase state, similar to liquid crystals [3, 8, 9].

As can be seen from Eq. (2), L^* grows when E_{k1} decreases, and at the same time the data points in Fig. 3 that deviated from the interpolating line must now fall closer to it. In this case, additional experimental data on the enthalpy of solid–solid phase transition that precedes melting are necessary to obtain a more accurate estimate of the decrease in E_{k1} and to calculate L^*.

In summary, we note that the discussed effect—generation, in small particles, of intermediate phase states that are not observed typically in corresponding bulk materials—enabled us to point to a similarity between LCMCs and high molecular weight polymers. Due to the presence of the first-order solid–solid (structural) phase transition in the LCMCs as a component of the melting process, we will be able to analyze the kinetics of new phase nucleation during melting and to study the interface expansion.

REFERENCES

1. V. M. Egorov and V. A. Marikhin, Phys. Solid State **58**, 2574 (2016).
2. V. M. Egorov, V. A. Marikhin, L. P. Myasnikova, and P. N. Yakushev, Phys. Solid State **59**, 2070 (2017).
3. V. M. Egorov, V. A. Marikhin, and L. P. Myasnikova, Phys. Solid State **50**, 126 (2008).
4. V. M. Egorov, V. A. Marikhin, and L. P. Myasnikova, Polymer Sci., Ser. A **48**, 1270 (2006).
5. V. M. Egorov, V. A. Marikhin, L. P. Myasnikova, and N. Nakamura, Phys. Solid State **51**, 2129 (2009).
6. V. M. Egorov, V. A. Marikhin, and L. P. Myasnikova, Polymer Sci., Ser. B **47**, 339 (2005).
7. V. M. Egorov, V. A. Marikhin, and L. P. Myasnikova, Polymer Sci., Ser. A **49**, 1366 (2007).
8. V. M. Egorov, V. A. Marikhin, and L. P. Myasnikova, Polymer Sci., Ser. A **53**, 906 (2011).
9. V. M. Egorov, V. A. Marikhin, and L. P. Myasnikova, Phys. Solid State **55**, 1057 (2013).
10. N. T. Gladkikh, S. V. Dukarov, A. P. Kryshtal', V. I. Larin, V. N. Sukhov, and S. I. Bogatyrenko, *Surface Phenomena and Phase Transformations in Condensed Films* (Khark. Nats. Univ. im. V. N. Karazina, Khar'kov, 2004) [in Russian].
11. A. I. Gusev, *Nanomaterials, Nanostructures, Nanotechnologies* (Nauka, Moscow, 2007) [in Russian].
12. A. I. Gusev and A. A. Rempel, *Nanocrystalline Materials* (Cambridge Int. Sci. Publ., Cambridge, 2004).
13. V. M. Egorov and V. A. Marikhin, Phys. Solid State **58**, 2353 (2016).
14. B. N. Rolov and V. E. Yurkevich, *Physics of Diffused Phase Transitions* (Rostov. Univ., Rostov-on-Don, 1983) [in Russian].
15. G. A. Malygin, Phys. Usp. **44**, 173 (2001).
16. A. A. Askadskii, L. K. Kolmakova, A. A. Tager, G. L. Slonimskii, and V. V. Korshak, Vysokomol. Soedin., Ser. A **19**, 1004 (1977).
17. J. I. Lauritzen, and J. D. Hoffman, J. Res. Natl. Bur. Stand. (U. S.) A **64**, 73 (1960).
18. J. D. Hoffman and J. J. Weeks, J. Res. Natl. Bur. Stand. (U. S.) A **66**, 13 (1962).
19. B. Wunderlich, *Macromolecular Physics*, Vol. 3: *Crystal Melting* (Academic, New York, 1976).

Translated by A. Kukharuk